*Korean J. Chem. Eng.*, **25**(1), 59-63 (2008)

# A semi-empirical model for the air oxidation kinetics of $UO_2$

**Byung Heung Park† and Chung-Seok Seo**

Korea Atomic Energy Research Institute, 150-1 Dukjin-dong, 1045 Daedeokdaero, Yuseong, Daejeon 305-353, Korea
(*Received 17 May 2007 • accepted 12 June 2007*)

**Abstract**−$UO_2$ is readily oxidized to $U_3O_8$ at a high temperature, and this reaction has received considerable attention in the field of nuclear fuel cycles. A voloxidation process which makes use of the characteristics of a $UO_2$ oxidation has been developed to treat the spent fuels produced by irradiation of $UO_2$. In this work, semi-empirical kinetic models to describe the sigmoidal behavior of a $UO_2$ oxidation were selected and compared in order to obtain a kinetic expression with different temperatures. Two basic approaches of a nucleation-and-growth model and an autocatalytic reaction model were adequate enough to describe the S-shaped oxidation behavior, and an equation to correlate the model parameters with the temperature was introduced. The calculation results of the two models satisfy the experimental data for $UO_2$ spheres and the activation energy of a reaction rate constant was evaluated. The models were also adopted as a surface reaction time term for a $UO_2$ pellet.

Key words: $UO_2$, Oxidation, Kinetics, Model, Voloxidation

## INTRODUCTION

Uranium dioxide is used as a fuel for nuclear power generation in light and heavy water reactors since $UO_2$ is a stable ceramic material with a high melting point (≅2,800 ºC) and, accordingly, the chemical form of irradiated fuels where $UO_2$ takes more than 95% can be expressed as $MO_2$. The mechanism of $UO_2$ oxidation has been investigated to understand the long-term behavior of disposed spent fuel (SF) for dry storage [1-3], and a process for the oxidation of $UO_2$ has been developed for containment of the tritium emissions from nuclear fuel reprocessing facilities by researchers at the Oak Ridge National Laboratory (ORNL) [4,5] and others [6] by the name of "voloxidation" which is a combined word from "volatilization" and "oxidation" to account for the separation of volatile fission products and the oxidation of $UO_2$, respectively. Recently, a voloxidation process was adopted as a "head-end" process step for an electrolytic reduction process [7-9] in an advanced spent fuel conditioning process (ACP) which has been proposed and developed at the Korea Atomic Energy Research Institute (KAERI). A density difference as a result of an oxidation transforms a pellet form of an SF into a powder form and, as a consequence, produces reactants with a large surface area for an electrolytic reduction process. Some of the volatile fission products such as Kr and Xe are removed from the SF by a voloxidation under an air-blowing condition which reduces the level of the radioactivity in the following process.

A stable $UO_2$ changes into $U_3O_8$ under an oxidizing atmosphere at high temperatures. The kinetics and oxidation mechanism of this reaction have not been clarified as yet although there have been some experimental studies [1,10-12] on this reaction. The sigmoidal behavior of $UO_2$ oxidation was observed and it was understood as a result of two successive steps of $UO_2$ to $U_4O_9/U_3O_7$ followed by $U_4O_9/U_3O_7$ to $U_3O_8$ [13,14]. However, a differential thermal analysis study showed that the entire oxidation proceeded in a single stage when the temperature rose rapidly [12]. Recently, Jeong et al. [15] proposed a new kinetic model for this reaction including a diffusion of oxygen through a film and a product layer. Moreover, the Johnson-Mehl equation [2,11,14] for nucleation and growth was proven to be compatible with the diffusion terms by Jeong and coauthors [15]. The kinetic expression of Jeong et al. [15] was derived by combining the resistances of film diffusion and product layer diffusion.

The Johnson-Mehl equation of the nucleation and growth model is expressed as a Weibull distribution function. However, applications of this equation for a wide range of temperatures have not been investigated. Moreover, the authors noticed that another model for the kinetics of $UO_2$ oxidation can be developed on the basis of a Gompertz function for describing the characteristic sigmoidal behavior.

An understanding of the $UO_2$ oxidation kinetics is indispensable for designing a voloxidizer and determining the operation conditions for a voloxidation process. However, the reaction data for a voloxidation condition are not sufficient to correlate a model. Therefore, the aim of this study is to provide a practical model for describing the oxidation behavior of $UO_2$ for the voloxidation process by using the available reaction data. In this study, two of the currently available models for an oxidation of $UO_2$ were applied to describe the conversion behavior of $UO_2$ with different reaction temperatures.

## KINETIC MODELS

The oxidation of $UO_2$ occurs by reacting it with oxygen gas in air and it can be represented as the following equation:

$$3UO_2(s)+O_2(g)\rightarrow U_3O_8(s) \quad (1)$$

The densities of crystalline $UO_2$ and $U_3O_8$ are 10.97 and 8.38 g/cm$^3$, respectively. Therefore, the reacted part of $UO_2$ swells because of the density difference of the two oxides and pathways are opened for the oxygen gas to reach the unreacted $UO_2$ core. As the reaction proceeds, the thickness of a product layer does not increase in pro-

†To whom correspondence should be addressed.
E-mail: bhpark@kaeri.re.kr

portion to the extent of the reaction because the produced $U_3O_8$ falls from the core in the form of a fine powder.

**1. Nucleation and Growth Model (NGM)**

The rate of formation of $U_3O_8$ from $UO_2$ is generally described by a nucleation-and-growth model [14]. An oxidation rate increases gradually after a low initial reaction rate, and then it decreases as the reaction approaches its completion. This oxidation behavior results in an S-shaped curve with respect to a reaction time. By assuming that $UO_2$ oxidation takes place by a single reaction of Eq. (1) and a distribution of the reaction times is governed by a generalized 3-parameter Weibull distribution function of the following Eq. (2), the conversion can be written by using the cumulative Weibull distribution function (Eq. (3)):

$$f(t)=\frac{k}{\lambda}\left(\frac{t-\theta}{\lambda}\right)^{k-1}\exp\left[-\left(\frac{t-\theta}{\lambda}\right)^{k}\right] \quad (2)$$

$$X(t)=1-\exp\left[-\left(\frac{t-\theta}{\lambda}\right)^{k}\right] \quad (3)$$

where, k, $\lambda$, and $\theta$ are the shape, scalar and location parameters of the Weibull distribution function, respectively. A numerical expression of the nucleation-and-growth model is identical to the Weibull distribution function of Eq. (2) which is based on a distribution of the active sites on a reactant.

Actually, there is no oxidized surface on $UO_2$ reactants when oxidation has just taken place. Therefore, the oxidized fraction should be zero at an initial state, which means a location parameter for Eqs. (2) and (3) is unnecessary and the oxidized fraction is expressed as a reduced-parameter equation as follows:

$$X(t)=1-\exp\left[-\left(\frac{t}{\lambda}\right)^{k}\right] \quad (4)$$

Eq. (4) is the form of a 2-parameter cumulative Weibull distribution function and will be written as NGM in this paper, since it has the same numerical expression as a nucleation and growth model.

In the NGM, the free energies of the reactive centers for a $UO_2$ oxidation are considered to be distributed by a statistical probability, and the concentration of oxygen is assumed to remain constant during the reaction.

**2. Autocatalytic Reaction Model (ARM)**

Sigmoidal behavior is also found in the characteristic curves from autocatalytic reactions. The rate equation of an autocatalytic reaction model which includes nucleation, growth, and coalescence processes has been successfully applied to the analysis of an oxidation of Si [16]. In the food industry, the autocatalytic reaction is of importance and models for the S-shaped autocatalytic behavior have been proposed. Quintas et al. [17] modified a logistic and a Gompertz equation to describe the reaction with kinetic parameters for the autocatalytic behavior of a sucrose thermal degradation. The Gompertz equation is an empirical equation that has more commonly been used to describe various phenomena and a Gompertz-type equation for the $UO_2$ oxidation is mathematically given by the following equation:

$$X(t)=\exp\left[-\exp\left(-\frac{(t-\theta)}{b}\right)\right] \quad (5)$$

where, $\theta$ and b are shape parameters in the Gompertz equation. It is also assumed that the concentration of oxygen is stable throughout the oxidation.

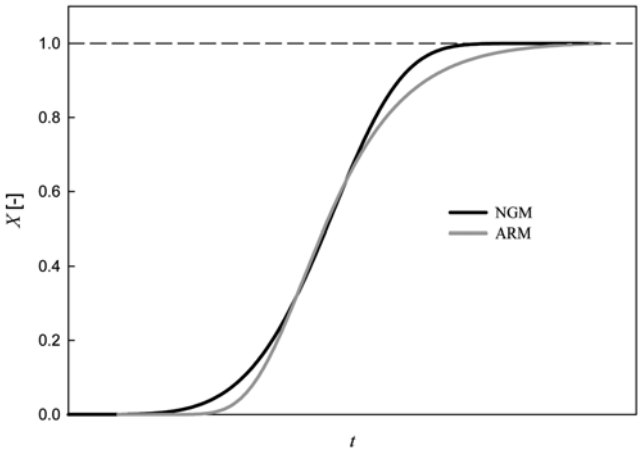


**Fig. 1. Oxidation behavior of NGM and ARM.**

**3. Oxidation Behavior and Temperature Dependency of NGM and ARM**

Oxidation tendencies of the two models are compared in Fig. 1. The two models show a sigmoidal behavior as expected and NGM describes an earlier start and completion of an oxidation than ARM. In the highest oxidation rate region, the two models behave almost identically and the maximum reaction rates, which are the slopes of the steepest tangents to the oxidation curves, are also almost identical.

Both NGM and ARM have two parameters at a given temperature. The two models were correlated well with the experimental data of a sigmoidal behavior at a given temperature. However, the parameters which were determined to minimize the deviations of the models from the experimental data were different at other temperature conditions. Therefore, to extend the models to a certain temperature range, a temperature dependency is required. In this work, the authors found that the following equation was appropriate to correlate the model parameters with different temperatures:

$$C=C_1(1+C_2/T+C_3\ln T) \quad (C=\lambda, k, \theta, b) \quad (6)$$

where, T in Eq. (6) is the temperature of °C and $C_i$(i=1, 2, 3) are the temperature coefficients of a parameter C($C=\lambda$, k, $\theta$, b).

## CALCULATION RESULTS AND DISCUSSIONS

**1. $UO_2$ Sphere**

The two models were correlated with the reported experimental data of natural $UO_2$ spheres [11] of which the mean diameters were 120 mm. Calculation results for the oxidation are presented in Fig. 2. Temperature coefficients of the model parameters and deviations from the experimental data are listed in Table 1 for both NGM and ARM.

The absolute average deviations (AADs) in Table 1 show that the two models describe the oxidation of $UO_2$ spheres satisfactorily. For a spherical $UO_2$, NGM is more accurate than ARM at the early stage of an oxidation. However, at the completion stage, ARM describes the oxidation behavior more correctly than NGM, and this

**Table 1. Temperature coefficients and deviations from the experimental data**

| Model | $\lambda_1$ | $\lambda_2$ | $\lambda_3$ | $k_1$ | $k_2$ | $k_3$ | AAD* |
|---|---|---|---|---|---|---|---|
| | $\theta_1$ | $\theta_2$ | $\theta_3$ | $b_1$ | $b_2$ | $b_3$ | |
| NGM | $1.4035\times10^4$ | −30.994 | −0.15360 | $8.3118\times10^2$ | −47.596 | −0.14668 | 0.0658 |
| ARM | $1.5608\times10^4$ | −36.043 | −0.15168 | $-1.9743\times10^3$ | −78.353 | −0.13560 | 0.0673 |

*$AAD=1/N\Sigma|X_{i,data}-X_{i,calc}|$

makes the overall accuracy of NGM and ARM similar. Considering a reactor design viewpoint, the completion stage is more important than an early state in order to decide on the reaction time for $UO_2$ oxidation.

The following reaction expression represents a general heterogeneous reaction:

$$A(fluid)+\nu_B B(solid)\rightarrow P(solid) \quad (7)$$

When a chemical reaction controls Eq. (7), a gas film and an ash layer diffusion can be neglected and the progress of the reaction is governed by the following rate of a reaction which is based on a unit surface of an unreacted core [19].

$$-\rho_B\frac{dr_C}{dt}=\nu_B k_s C_{Ag} \quad (8)$$

where $\rho_B$, $r_C$, $\nu_B$, and $k_s$ are the molar density of a solid reactant, the radius of an unreacted core, a stoichiometric number, and the first-order rate constant, respectively. The molar concentration of a gaseous reactant in the gas phase is denoted as $C_{Ag}$ in Eq. (8). The fractional conversion ($X_B$) in a spherical reactant with a radius of r can be written by an unreacted volume ratio as follows;

$$1-X_B=\left(\frac{r_C}{r}\right)^3 \quad (9)$$

Combining Eq. (8) with Eq. (9), we can obtain the following expression for the rate of a fractional conversion:

$$\frac{dX_B}{dt}=\frac{3\nu_B k_s}{r\rho_B}C_{Ag}(1-X_B)^{2/3} \quad (10)$$

Using the derivatives of Eqs. (4) and (5), the following equations for the reaction rate constant can be arranged from Eq. (10) for NGM (Eq. (11)) and ARM (Eq. (12)).

$$k_s(NGM)=\frac{r\rho_B}{3\nu_B C_{Ag}}(1-X_B)^{1/3}\frac{k}{\lambda}[-\ln(1-X_B)]^{(k-1)/k} \quad (11)$$

$$k_s(ARM)=\frac{r\rho_B}{3\nu_B C_{Ag}}\frac{X_B\ln(1/X_B)}{b(1-X_B)^{2/3}} \quad (12)$$

As derived in Eqs. (11) and (12), the reaction rate constant depends on the fractional conversion as well as the temperature. An Arrhenius type of an expression for the reaction rate is generally adopted to obtain activation energies as follows:

$$k_s=k_{s0}\exp(-E_\alpha/RT) \quad (13)$$

where $k_{s0}$ (cm/min) is the frequency factor of the reaction rate constant. $E_\alpha$ (kJ/mol), R (J/mol/K), and T (K) are the activation energy, the universe gas constant, and the absolute temperature, respectively.

Figs. 3 and 4 present the Arrhenius type plots of the reaction rates

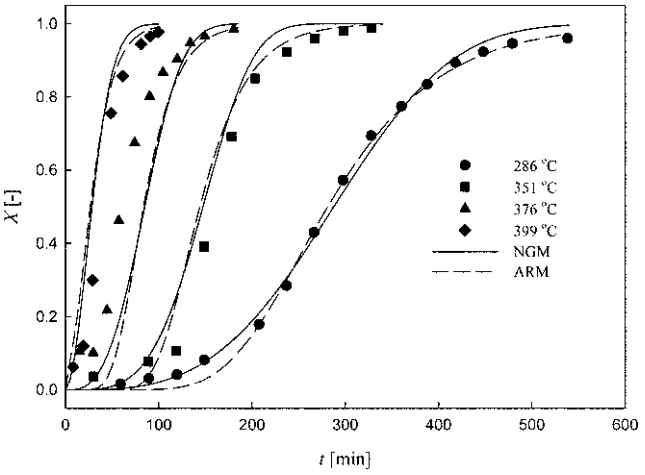


**Fig. 2. Calculation results for an isothermal oxidation of unirradiated natural $UO_2$ spheres.**

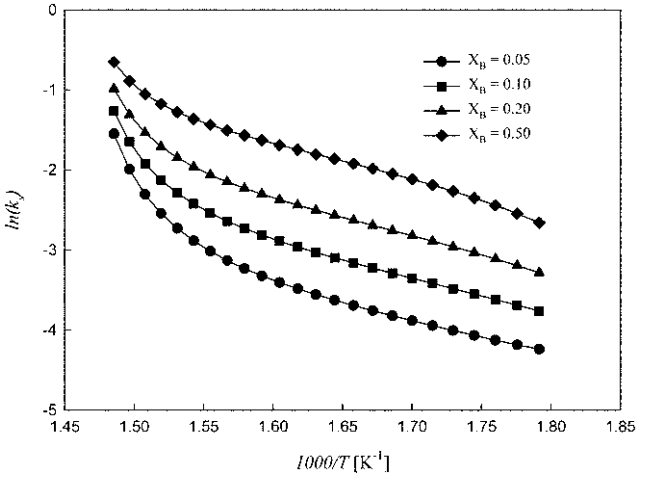


**Fig. 3. Arrhenius plots of the reaction rate constant using NGM for an oxidation of an unirradiated natural $UO_2$ sphere.**

for NGM and ARM, respectively, in case that the fractions of the oxidation are 0.05, 0.10, 0.20, and 0.50 from natural $UO_2$ spheres. The slopes of the plots in Figs. 3 and 4 present the activation energies for the reaction. As shown in Fig. 3, plots for NGM exhibit a change of the activation energy at a given oxidation fraction, while the linearity of the plots from ARM gives a constant activation energy at a given oxidation fraction as presented in Fig. 4. The evaluated activation energy of the natural $UO_2$ spheres from NGM increases from 42.08 kJ/mol at 285-365 °C to 127.43-242.18 kJ/mol, and then decreases with an increasing oxidation fraction at 375-

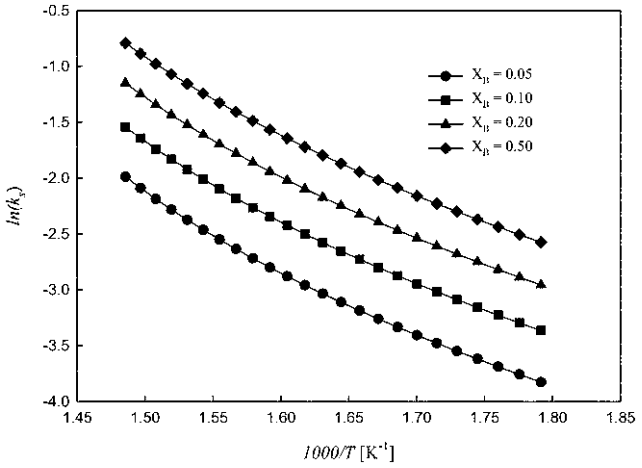


**Fig. 4. Arrhenius plots of the reaction rate constant using ARM for an oxidation of an unirradiated natural $UO_2$ sphere.**

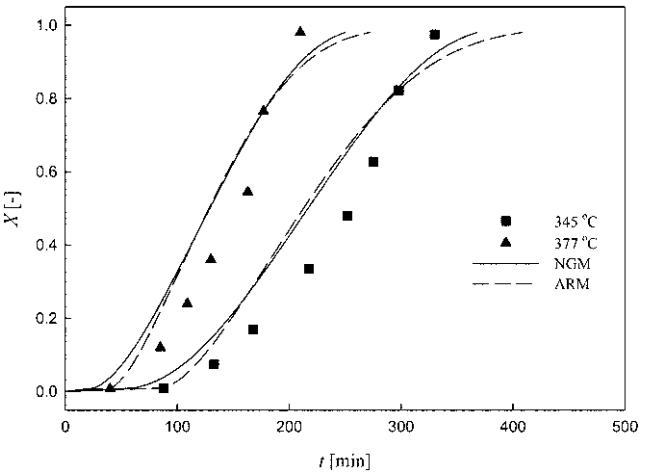


**Fig. 5. Calculation results for an isothermal oxidation of unirradiated natural $UO_2$ pellets.**

400 °C and that from ARM is 48.57 kJ/mol at 285-400 °C. The evaluated activation energies are lower than the values of Kang et al. [18] who used sintered particles of 8.5 mm in diameter and 1.4 mm in thickness. The size and the shape of samples are thought to affect the oxidation behavior [14], and other effects such as a diffusion of gas at different sizes and shapes seem to be included in the activation energy of the particle samples.

**2. $UO_2$ Pellet**

The reaction time for the oxidation of a large $UO_2$ particle can be divided into three parts of a gas film diffusion, an ash layer diffusion and a surface reaction to take into account the individual processes involved in the overall process. If the additive relation is assumed [15], the total reaction time can be expressed as a summation of the times for gas film diffusion ($t_{film\ diff}$), ash layer diffusion ($t_{ash\ diff}$), and surface reaction ($t_{rx}$) as follows:

$$t=t_{film\ diff}+t_{ash\ diff}+t_{rx} \tag{14}$$

For a cylindrical particle of constant size during a reaction, the diffusion times in a gas film and an ash layer can be obtained by Eqs. (14) and (15), respectively [19]:

$$t_{film\ diff}=\frac{\rho_B r}{2\nu_B k_g C_{Ag}}X_B \tag{14}$$

$$t_{ash\ diff}=\frac{\rho_B r^2}{4\nu_B D_e C_{Ag}}[X_B+(1-X_B)\ln(1-X_B)] \tag{15}$$

where, $k_g$ and $D_e$ are the mass transfer coefficient and the effective diffusion coefficient of a gaseous reactant in an ash layer, respectively. For the surface reaction time, we can simply rearrange the proposed kinetic equations of Eqs. (4) and (5).

$$t_{rx}(\mathrm{NGM})=\lambda[-\ln(1-X_B)]^{(1/k)} \tag{16}$$

$$t_{rx}(\mathrm{ARM})=\theta-b\ln(-\ln X_B) \tag{17}$$

Finally, two expressions for the reaction time can be derived by adding Eqs. (14) and (15) to Eq. (16) or Eq. (17).

The obtained reaction time expressions for the $UO_2$ pellet were used to describe the oxidation behavior of a $UO_2$ pellet of 1.4 cm in diameter [1]; the result is given in Fig. 5 at two different temperatures. Using the parameters listed in Table 1, two additional parameters for diffusions were determined as 13.58 (cm/min) for $k_g$ and 78.42 ($cm^2$/min) for $D_e$. The constants $k_g$ and $D_e$ and the same values of $k_g$ and $D_e$ are used for both models. As shown in Fig. 5, the calculation results were acceptable when considering a number of variables such as a shape and an air flowing rate that can affect the rates at which $UO_2$ will oxidize.

## CONCLUSIONS

The kinetics of $UO_2$ oxidation follows a sigmoidal relation with time under an isothermal condition. To model this behavior, for practical purposes, a nucleation and growth model (NGM) which is based on a Weibull distribution function and an autocatalytic reaction model (ARM) in the form of a Gompertz equation were compared for the oxidation of $UO_2$. To describe its oxidation behavior with respect to the temperature, the parameters of the two models were correlated with the proposed equation in this study.

The two models satisfactorily depicted the oxidation behavior of spherical $UO_2$. NGM was better for an early stage of the oxidation; however, ARM predicted the completion stage of the oxidation more accurately than NGM. The activation energy of the reaction rate constant which was derived by an Arrhenius type equation was constant for ARM, while it increased for NGM with the temperature. It is expected that a semi-empirical reaction model based on ARM could be applicable to the design of a voloxidizer and to establish the operational conditions of a voloxidation process, since ARM is simple and provides accurate results at the completion stage of an oxidation with constant activation energy.

Kinetic expressions were adopted to obtain a mathematical formula for the oxidation of a pellet type $UO_2$ under the assumption that the reaction time is composed of additive terms for gas film diffusion, ash layer diffusion, and surface reaction. The accuracy for the $UO_2$ pellet oxidation is not as satisfactory as micro-spherical $UO_2$ oxidation. However, a model based on a clarified reaction mechanism with respect to the respective reaction conditions could improve the accuracy by adding a corresponding term to the proposed equation in this work. Moreover, the proposed semi-empiri-

cal equation could be developed further to describe SF oxidation for practical purposes when the behavior and the effects of the fission products in an SF are not established.

## REFERENCES


1. D. G. Boase and T. T. Vandergraaf, *Nucl. Technol.*, **32**, 60 (1977).
2. J.-W. Choi, R. J. McEachern, P. Talyor and D. D. Wood, *J. Nucl. Mater.*, **230**, 250 (1996).
3. G.-S. You, K.-S. Kim, D.-K. Kim and S.-G. Ro, *J. Nucl. Mater.*, **277**, 325 (2000).
4. E. L. Nicholson, ORNL Report, ORNL/CF-76/65, Oak Ridge National Laboratory, Oak Ridge, U.S.A. (1976).
5. W. S. Groenier, ORNL Report, ORNL/CF-77/67, Oak Ridge National Laboratory, Oak Ridge, U.S.A. (1977).
6. G. Uchiyama, M. Kitamura, K. Yamazaki, S. Torikai, S. Sugikawa, M. Maeda and T. Tsujino, *Radioactive Waste Management and the Nuclear Fuel Cycle*, **17**, 63 (1992).
7. S. M. Jeong, S.-B. Park, S.-S. Hong, C.-S. Seo and S.-W. Park, *J. Radioanal. Nucl. Chem.*, **268**, 349 (2006).
8. S. B. Park, B. H. Park, S. M. Jeong, J. M. Hur, C.-S. Seo, S.-H. Choi and S. W. Park, *J. Radioanal. Nucl. Chem.*, **268**, 489 (2006).
9. B. H. Park, S. B. Park, S. M. Jeong, C.-S. Seo and S.-W. Park, *J. Radioanal. Nucl. Chem.*, **270**, 575 (2006).
10. K. A. Peakallr and J. E. Antill, *J. Nucl. Mater.*, **2**, 194 (1960).
11. K. T. Harrison, C. Padgett and K. T. Scott, *J. Nucl. Mater.*, **23**, 121 (1967).
12. H. Ohashi, E. Noda and T. Morozumi, *J. Nucl. Sci. Technol.*, **11**, 445 (1974).
13. R. J. McEachern, *J. Nucl. Mater.*, **245**, 238 (1997).
14. R. J. McEachern and P. Taylor, *J. Nucl. Mater.*, **254**, 87 (1998).
15. S. M. Jeong, K.-C. Kwon, B. H. Park and C.-S. Seo, *React. Kinet. Catal. Lett.*, **89**, 269 (2006).
16. M. Suemitsu, H. Togashi and T. Abe, *Thin Solid Films*, **428**, 83 (2003).
17. M. Quintas, T. R. S. Brandão and C. L. M. Silva, *J. Food Eng.*, **78**, 537 (2007).
18. K. H. Kang, S. H. Na, K. C. Song, S. H. Lee and S. W. Kim, *Thermochim. Acta*, **455**, 129 (2007).
19. O. Levenspiel, *Chemical reaction engineering*, 2nd ed., Wiley, New York (1972).